constructed a stochastic population model, parameterized using the density-dependent relationships shown in Fig. 2. Our model simultaneously considered male and female densities and potential harvests in two neighbouring populations that were small enough for differences in the culling regimes imposed on each population to produce local differences in sex-specific emigration and immigration, as well as in mortality. We assumed that both populations were biologically identical and were subject to correlated environmental variability: relaxation of these assumptions was unlikely to affect the direction of predicted trends. Vital rates used were initially calculated deterministically as $R_j = 1/[1 + \exp(-a + bD)]$, where D was the density of mature females (age classes 3 and above), j was the age class and a and b were constants. Sex ratio at birth was calculated as $m = 64.3 - 0.748D$, where m is the percentage of males. Vital rates were subsequently altered to include variability and correlations as follows: for emigration rates, sex ratio at birth and female mortality, $\rho_j = R_j + z\sigma_j$; for fecundity and male mortality, $\rho_j = R_j + \sigma_j z\sqrt{1 - r^2} + r\sigma_j A$, where ρ_j was the stochastic rate, z is a z-value (see below), r was the correlation coefficient between this rate and 3+ female mortality, σ_j^2 is the standard deviation of the vital rate and A was the average value of the z values for 3+ female mortality rates. The values of r were −0.452 for fecundity and 0.522 for male mortality. The z values for population 1 were simple standardized normal deviates. Those for population 2 were calculated as: $z_2 = Z_2\sqrt{1 - r^2} + rz_1$, where Z_2 was the original z value, r was the correlation between populations, and z_1 was the z-value calculated for the equivalent age class and vital rate for population 1. The value of r was 0.7.

Received 2 August; accepted 20 November 2001.

1. Klein, D. R. The introduction, increase, and crash of reindeer on St. Matthew Island. *J. Wildl. Mgmt* **32,** 350–367 (1968).
2. Flook, D. R. A study of sex differential mortality in the survival of wapiti. (Canadian Wildlife Service Report Series, Ottowa, 1970).
3. Clutton-Brock, T. H., Price, O. F., Albon, S. D. & Jewell, P. A. Persistent instability and population regulation in Soay sheep. *J. Anim. Ecol.* **60,** 593–608 (1991).
4. Clutton-Brock, T. H., Guinness, F. E. & Albon, S. D. *Red Deer: Behaviour and Ecology of Two Sexes* (Univ. Edinburgh Press, Edinburgh, 1982).
5. Clutton-Brock, T. H. & Albon, S. D. *Red Deer in the Highlands* (Blackwell Scientific, Oxford, 1989).
6. Clutton-Brock, T. H., Major, M. & Guinness, F. E. Population regulation in male and female red deer. *J. Anim. Ecol.* **54,** 831–846 (1985).
7. Clutton-Brock, T. H. & Lonergan, M. E. Culling regimes and sex ratio biases in Highland red deer. *J. Appl. Ecol.* **31,** 521–527 (1994).
8. Bryden, J. M. in *The Next Twenty Years* 1–41 (Red Deer Commission, Inverness, 1979).
9. Jarvis, E. *The Red Deer Industry* (The Scottish Landowner's Federation, Edinburgh, 1978/9).
10. Milne, J. A., Birch, C. P. D., Hester, A. J., Armstrong, H. & Robinson, A. The impact of vertebrate herbivores on the natural vegetation of the Scottish upland: a review. 1–127 (Report no. 95, Scottish National Heritage, Edinburgh 1998).
11. Lowe, V. P. W. Population dynamics of the red deer (*Cervus elaphus* L.) on Rhum. *J. Anim. Ecol.* **38,** 425–457 (1969).
12. Lowe, V. P. W. in *The Scientific Management of Animal and Plant Communities for Conservation* (eds Duffey, E. & Watt, A. S.) 437–445 (Blackwell, Oxford, 1971).
13. Kruuk, L. E. B., Clutton-Brock, T. H., Albon, S. D., Pemberton, J. M. & Guinness, F. E. Population density affects sex ratio variation in red deer. *Nature* **399,** 459–461 (1999).
14. Clutton-Brock, T. H., Albon, S. D. & Guinness, F. E. Parental investment and sex differences in juvenile mortality in birds and mammals. *Nature* **313,** 131–133 (1985).
15. Clutton-Brock, T. H., Rose, K. E. & Guinness, F. E. Density-related changes in sexual selection in red deer. *Proc. R. Soc. Lond. B* **264,** 1509–1516 (1997).
16. Charles, W. N., McCowan, D. & East, K. Selection of upland swards by red deer *Cervus elaphus* L. on Rhum. *J. Appl. Ecol.* **14,** 55–64 (1977).
17. Clutton-Brock, T. H., Iason, G. R. & Guinness, F. E. Sexual segregation and density-related changes in habitat use in male and female red deer (*Cervus elaphus*). *J. Zool.* **211,** 275–289 (1987).
18. Conradt, L., Clutton-Brock, T. H. & Thomson, D. Habitat segregation in ungulates: are males forced into suboptimal habitats through indirect competition by females? *Oecologia* **119,** 367–377 (1999).
19. Mutch, W. E. S., Lockie, J. D. & Cooper, A. N. *The Red Deer in South Ross: a Report on Wildlife Management in the Scottish Highlands* (Department of Forestry and Natural Resources, Univ. Edinburgh, 1976).
20. Annual Report 2000–2001. (Deer Commission for Scotland, Inverness, 2001).
21. Langvatn, R. & Loison, A. Consequences of harvesting on age structure, sex ratio and population dynamics of red deer *Cervus elaphus* in central Norway. *Wildl. Biol.* **5,** 213–223 (1999).
22. Mitchell, B., Staines, B. W. & Welch, D. *Ecology of Red Deer: a Research Review Relevant to their Management in Scotland* (Institute of Terrestrial Ecology, Cambridge, 1977).
23. Conradt, L., Clutton-Brock, T. H. & Guinness, F. E. Sex differences in weather sensitivity as cause of habitat segregation in red deer (*Cervus elaphus* L.). *Anim. Behav.* **59,** 1049–1060 (2000).
24. Osborne, B. C. Habitat use by red deer (*Cervus elaphus*) and hill sheep in the west Highlands. *J. Appl. Ecol.* **21,** 497–506 (1984).
25. Clutton-Brock, T. H. & Albon, S. D. Trial and error in the Highlands. *Nature* **358,** 11–12 (1992).
26. Sibbald, A. Using GPS to track wild red deer stags. *Deer* **11,** 524–529 (2000).
27. Buckland, S. T., Ahmadi, S., Staines, B. W., Gordon, I. J. & Youngson, R. W. Estimating the minimum population size that allows a given annual number of mature red deer stags to be culled sustainably. *J. Appl. Ecol.* **33,** 118–130 (1996).
28. Holloway, C. W. *The Effect of Red Deer and Other Animals on Naturally Regenerated Scots Pine.* Thesis, Univ. Aberdeen (1967).
29. McCullough, D. R., Pire, D. S., Whitmore, D. L., Mansfield, T. M. & Decker, R. H. Linked sex harvest strategy for big game management with a test case in black-tailed deer. *Wildl. Monog.* **112,** 1–41 (1990).
30. McCullough, D. R. Population manipulations of North American deer *Odocoileus* spp.: balancing high yield with sustainability. *Wildl. Biol.* **7,** 161–171 (2001).
31. Lubow, B. C., White, G. C. & Anderson, D. R. *J. Wildl. Mgmt* **60,** 787–796 (1996).

Acknowledgements

We thank F. E. Guinness, J. M. Pemberton and S. Albon for maintaining the long-term records in the north block of Rum; C. Duck, J. Kingsley, M. Twiss and C. Covey for collecting data on deer populations throughout Rum; R. Scott for organizing the manipulations of deer numbers on Rum; the staff of the Deer Commission for Scotland, especially C. MacLean and D. Youngson, for counting and culling deer on Rum; the SNH staff on Rum, especially M. Curry and D. Reed, for support in maintaining deer research on the island; S. D. Albon, I. Gordon, L. Conradt, L. Kruuk and S. Buckland for comments or help with these analyses; J. Taylor for providing Fig. 1b; and the NERC, the Deer Commission for Scotland, SNH and the Scottish Executive for funding.

Competing interests statement

The authors declare that they have no competing financial interests.

Correspondence and requests for materials should be addressed to T.H.C.-B. (e-mail: thcb@hermes.cam.ac.uk).

Influence of scene statistics on colour constancy

Jürgen Golz* & Donald I. A. MacLeod†

* *Department of Psychology, University of Kiel, 24098 Kiel, Germany*
† *Department of Psychology, University of California at San Diego, La Jolla, California 93093-0109, USA*

The light reflected from an object depends not only on the surface properties of this object but also on the illuminant. The same is true for the excitations of the photoreceptors, which serve as the basis for the perceived colour. However, our visual system has the ability to perceive constant surface colours despite changes in illumination[1]. The average chromaticity of the retinal image of a scene depends on the illumination, and thus might be used by the visual system to estimate the illumination and to modulate the correction that subserves colour constancy[2–4]. But this measure is not sufficient: a reddish scene under white light can produce the same mean stimulation as a neutral scene in red light. Higher order scene statistics—for example, the correlation between redness and luminance within the image—allow these cases to be distinguished. Here we report that the human visual system does exploit such a statistic when estimating the illuminant, and gives it a weight that is statistically appropriate for the natural environment.

A viewed surface reflects towards the observer's eye a characteristic fraction of the light that is cast on it; therefore, the stimulus for vision is the product of an illuminant component and a surface-reflectance component. Colour constancy requires the visual system to disentangle the surface-reflectance component from the product—in some sense discounting the illuminant colour—but the illuminant colour is not generally directly known. Problems like this are common in many aspects of visual perception. They are mathematically underdetermined, and additional constraints must be drawn from the regularities of the physical world to achieve a unique solution.

The mean chromaticity of the retinal image is often proposed to be an indicator of illuminant colour[2–4], because for a given scene this statistic varies systematically with changes in illumination. But in more realistic situations in which the scenes might change as well, this measure is ambiguous (Fig. 1a). To illustrate the ambiguity, consider the problem of distinguishing a predominantly reddish room under white light from a predominantly neutral one under reddish light. The mean chromaticity of the image received by the eye may be the same in these two cases, but human observers can

resolve the ambiguity and perceive correctly the reddish room as redder[1,5]. Even in scenes where obvious cues to the illuminant contained in the spatial structure of the image, such as specular reflections[6–9] and mutual reflections[10–12], are not available, the visual system can distinguish changes of the mean image chromaticity caused by illuminant changes from changes of the mean chromaticity caused by variations of the set of surfaces[13].

Here we offer an explanation for this ability: in such situations the distribution of intensity and chromaticity for the various surfaces within the retinal image yields additional evidence about the illuminant colour, and this evidence is exploited in human colour perception. In particular, as we show below, the interplay of surfaces and illuminants causes the correlation between surface redness and luminance within an image to be useful for resolving the image into its illuminant and surface components. Two examples of how this higher order statistic might resolve the ambiguity of the mean image chromaticity and thus improve the estimation of the illumination are shown in Fig. 1b and c.

We tested experimentally whether the luminance–redness correlation is used by the human visual system for estimating the illuminant colour. We analysed images of natural scenes[14] to find out how effective this and other higher order statistics are as information about the chromaticity of surfaces and illuminants in the natural environment.

For our experiments, we adopted stimuli that make it possible to vary independently various statistics (means, variances, correlations) of the distribution of colour and lightness within the display[15–17]. A circular test field was surrounded by random patterns of overlapping circles; these were of a fixed diameter but varied in colour and luminance to a degree that is typical of natural scenes[18]. We asked subjects to adjust the colour of the test field so that it appeared neutral grey. We chose a logarithmic cone excitation space (with the axes $\log r$, $\log b$ and log luminance) as our coordinate system. The chromaticity value r is the luminance-normalized excitation of cones sensitive to long wavelength, and b is the luminance-normalized excitation of cones sensitive to short wavelength[19]. An equal energy white has the values $r = 0.7$ and $b = 1.0$ ($\log r = -0.155$ and $\log b = 0.0$). Reds have higher r values, and greens have lower ones; blues have higher b values, and yellows have lower ones. Our experiments and analysis focused on the r coordinate, which varied over a range from distinctly greenish to distinctly reddish.

In our main experiment[14,20], we varied the luminance–redness correlation for the elements surrounding the test field—by introducing a linear dependence between $\log r$ and log luminance—independently of other statistics (means and variances). For a given condition, the chromaticity and luminance values for the circles in the surround were chosen to achieve a certain correlation value (−1.0, −0.8, 0.0, 0.8 or 1.0). If the perceived colour of the centre test spot was not influenced by the varied correlation, then the settings to make the test spot neutral grey would be the same for all five conditions, because the space-averaged chromaticities of the surrounds were the same. The surrounds would then be functionally equivalent with respect to the perceived colour of the centre test spot.

The results for subject DB are shown in Fig. 2a. For conditions

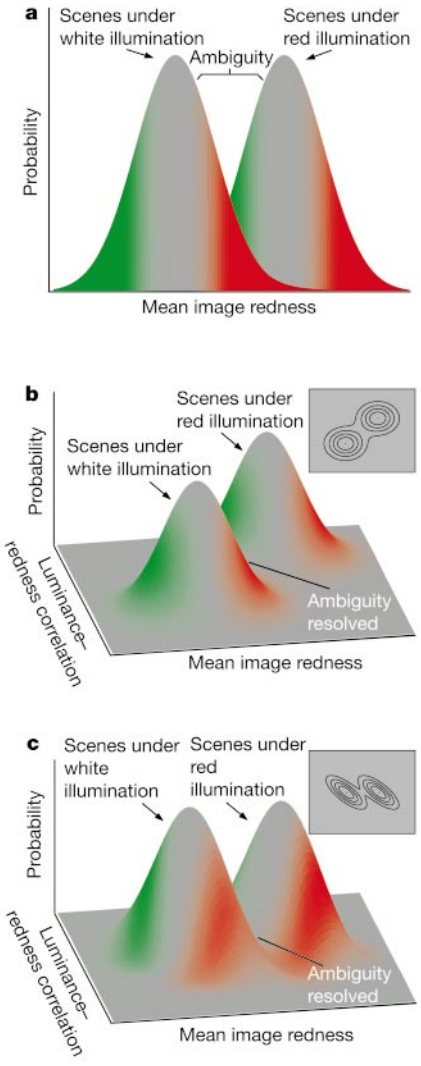

Figure 1 The ambiguity of the mean image chromaticity for estimating the illuminant, and two possibilities for resolving it using a higher order statistic (luminance–redness correlation). **a**, The same mean image chromaticity could result either from a reddish scene under white illumination or from a white scene under reddish illumination, because these two illuminants, applied to the given sample of scenes, generate overlapping distributions of mean image redness. **b**, Taking into account higher order statistics might resolve this ambiguity. In this example a higher order statistic, the luminance–redness correlation over the pixels of a single image, is increased for all images under the reddish illumination. Thus, a high luminance–redness correlation within the image would be evidence that the illuminant is reddish. Inset shows the corresponding view from above, depicting probability values by contour lines. **c**, Another way in which higher order scene statistics might separate the distributions of images from two different illuminants and thus reduce the ambiguity encountered in considering mean chromaticity alone. By evaluating both the mean and correlation of a particular image, an observer could estimate two unknowns: the degree of redness inherent in the objects making up the scene; and the redness of the light source that illuminates the scene. Inset shows the corresponding view from above, depicting probability values by contour lines.

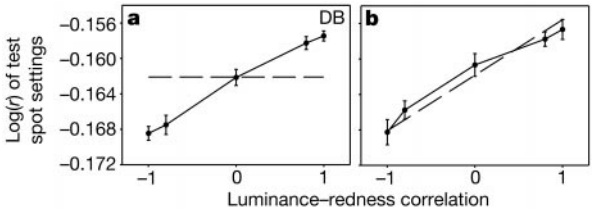

Figure 2 Dependence of centre test spot settings on the luminance–redness correlation within the surround. **a**, Results for subject DB. Filled circles are the mean $\log r$ values for perceptually achromatic test fields plotted as a function of the correlation between log luminance and $\log r$ for the five surround conditions; error bars represent ± 1 s.e.m. If the settings were not dependent on the correlation but only on the mean of the chromaticity of the surround, then settings would be the same for all conditions (horizontal dashed line). **b**, Average results for all subjects (circles) compared with predictions based on optimal use of the correlation statistic (dashed line). Error bars for the experimental results represent ± s.e.m. for subject variability.

with higher correlation between redness and luminance, a more reddish chromaticity was required to make the test field subjectively achromatic. The data for eight out of ten subjects tested were quantitatively similar and individually statistically significant ($P < 0.001$, linear trend test; two of these eight observers were also tested for correlation values of −0.4 and +0.4 and the results were in proportion to the other values). When the correlation between redness and luminance was positive, subjects selected a physically more reddish (higher log r) test field as neutral grey. Because higher log r values are associated with redder illumination of a physically neutral surface, this is the result that is expected if the observer infers a more reddish illumination in the case of a positive luminance–redness correlation and perceives neutral grey when a correspondingly reddish light stimulus is received from the test field. As shown in Fig. 2, this effect of the luminance–redness correlation is far from trivial; by comparison, a just noticeable difference in log r is only about 0.0004 (for example, see ref. 21).

Other work has provided evidence that the correction that subserves colour constancy is not governed merely by the space-averaged chromaticity[1,13,15–17,22–24], and some current colour constancy algorithms provide general frameworks for effects of this sort[25–28]. But so far only one group has made a specific suggestion about what statistic might also be diagnostic of the illuminant and found evidence that a reduced chromatic variance serves as a cue for a 'non-normal' illumination[15–17]. The luminance–redness correlation that we suggest makes it possible to resolve the retinal image into its illuminant and surface components over the whole range of typical daylights, as the following analysis shows.

To check how well chromatic statistics in images of natural scenes can support inferences about illuminant and surface colours, we used hyperspectral images of natural scenes[18]. To these 12 scenes, 4 daylight illuminations[29] were applied (correlated colour temperatures 4,000 K, 5,500 K, 8,500 K and 20,000 K; with increasing correlated colour temperature, the illuminants become less reddish (lower r values) and more bluish (higher b values)). We calculated several statistics (mean, variance, correlation, skewness) of the luminance and chromaticities for each illuminated scene. Of all the statistics that we evaluated besides the means, only the luminance–redness correlation was found to be useful for estimating the illumination colour.

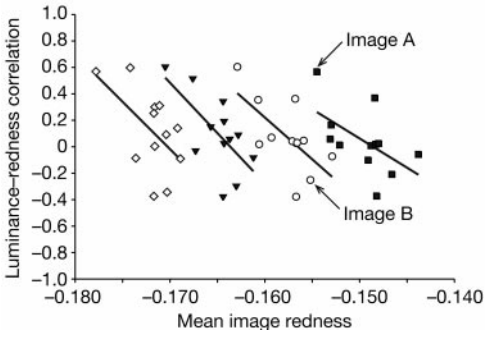

Figure 3 Luminance–redness correlation and mean redness of natural scenes under different illuminations. The vertical coordinate of each data point represents the correlation between pixel redness, log r and pixel luminance, log luminance, within an image of a scene under a particular illuminant. This correlation is plotted against mean image redness (mean of log r). The four clusters show data for 12 natural scenes under four different illuminants (filled squares, colour temperature 4,000 K; open circles, 5,500 K; filled triangles, 8,500 K, open diamonds, 20,000 K). The rank order for mean image redness of the 12 scenes stays almost unchanged under all four illuminants, indicating that scene redness can be roughly assessed by mean image redness for a given illuminant. For a given scene, the luminance–redness correlations are almost independent of illumination, but within each illuminant cluster they are more negative for the redder scenes, as shown by the negatively sloped regression lines. Thus, correlation and mean together separate the distributions of images resulting from different illuminants and make it possible to distinguish scene redness from illuminant redness, much as in the case of Fig. 1c. (The correlation between correlation (log r, log luminance) and mean (log r) for the four illuminant clusters are −0.555 (filled squares), −0.654 (open circles), −0.653 (filled triangles), −0.556 (open diamonds), in each case significantly different from zero, $P < 0.05$).

Although the experimental results suggest that the human visual system interprets a high luminance–redness correlation as a redder illuminant, the correlation alone is not an effective cue in determining the illuminant colour (Fig. 3). The correlations are almost independent of illumination. This measure can nevertheless resolve ambiguity, but more like in the case shown in Fig. 1c than in Fig. 1b; that is, when used together with the mean image redness, this measure separates the clusters of images from different illuminations (the four diagonally oriented clusters in Fig. 3) and thus permits the estimation of illumination colour.

For example, an image with a mean log r value of −0.155 could be a reddish scene under neutral light or a neutral (or even greenish) scene under reddish light (Fig. 3). But if the visual system takes into account the correlation between redness and luminance, it can distinguish between illumination redness and scene redness. The more positive the correlation, the greater the evidence for the redness of the illumination as opposed to redness of the scene. In Fig. 3, image A is with high probability a greenish scene under the reddish illuminant of 4,000 K whereas image B is likely to be a reddish scene that belongs to the cluster of the more neutral illuminant of 5,500 K.

The reason why the luminance–redness correlation can help in this way is that scene redness and illuminant redness affect the correlation differently. Because of the eye's spectral sensitivity, middle wavelengths contribute more to luminance than do short or long wavelengths. Under 'neutral' lighting, it is the neutral or moderately reddish and greenish pixels that reflect most middle-wavelength light, and which therefore have the highest luminance. In neutral or greenish scenes, surfaces that reflect predominantly long wavelengths and thus have lower luminance are rare. But in reddish scenes under neutral lighting, the eye's diminishing sensitivity at long wavelengths will discriminate against the most reddish pixels of a reddish scene, and these will therefore tend to be of much lower luminance. The luminance–redness correlation thus becomes more negative with more reddish scenes, as the sloped regression lines in Fig. 3 show.

No comparable effect occurs if it is not the scene but the light that is reddish. In this case, the low luminosity of reds is counterbalanced by the illuminant's greater energy at long wavelengths. Reddish surfaces reflect a larger proportion of long-wavelength than of short-wavelength light. Thus, when the illuminant becomes reddish the reddish surfaces will be more luminous relative to other colours in the scene, owing to the better overlap of their spectral reflectances with the spectral range in which the illuminant has its highest power.

Thus, reddish scenes but not reddish illuminants generate images with negative luminance–redness correlations. By evaluating both mean and correlation—two independent quantities—an observer can estimate two unknowns: the predominant colour (in this case, the degree of redness) inherent in the objects making up the scene; and the redness of the light source that illuminates the scene. In this way, the ambiguity encountered in considering mean chromaticity alone can be resolved.

How much weight should a smart visual system give to the correlation between redness and luminance in estimating the illumination? To answer this question for our simulated world of natural scenes under different illuminations, we calculated a maximum likelihood estimate for the chromaticity of the illumination given the mean and correlation value of an image (see Methods). Figure 2b illustrates the results in terms of how an optimal observer, adopting this maximum likelihood estimate, would have reacted to the stimuli of our experiment. The dashed line is a parameter-free

prediction for the test field chromaticity that would appear neutral grey, which is based on the hypothesis that optimal weight is given to the correlation measure in estimating the illuminant. For comparison, the circles in Fig. 2b show the test field settings that appeared neutral by experiment. The size of the observed effect of this statistic on colour perception is roughly consistent with optimal computation. □

Methods

Experiments

Stimuli consisted of a random pattern of overlapping circles (each 3.6° in diameter) covering the whole display area of 41° (height) and 53° (width). The chromaticity distributions of these displays, set by assigning different colours to the circles, were -0.16 ± 0.01 and -0.14 ± 0.06 (mean ± s.d.; $\log r$ and $\log b$). Luminance was 7 ± 3.6 cd m^{-2} (mean ± s.d.). The statistics of the correlation between $\log r$ and log luminance were −1.0, −0.8, 0.0, 0.8 and 1.0 for the five conditions, whereas the correlation between $\log b$ and log luminance was always 0.0, and the correlation between $\log b$ and $\log r$ was always −0.137. The test spot was a circle in the centre of the display, which was also 3.6° in diameter but on top of all other circles in this area. The luminance of the test spot was held constant at 7 cd m^{-2} while the subjects adjusted its chromaticity in the ($\log r$, $\log b$) plane by means of a trackball to make it look grey.

We presented stimuli on a carefully calibrated 17-inch (43-cm) Mitsubishi Diamond Pro monitor driven by a CRS VSG2/4f graphic board with 15 bits resolution per gun. Subject viewed the stimuli from a distance of 55 cm in a dark room through a tunnel of black velvet to exclude any other light sources or reflections. To achieve an equilibrium state of adaptation, subjects had to adapt to each display for at least 100 s.

Ten subjects aged between 11 and 34 years participated in two 1-h sessions making six settings per condition. All participants except one (J.G.) were naive to the purpose of the experiment. All had normal or corrected-to-normal vision and showed no colour vision deficiency, as tested by Ishihara's test plates.

Theoretical analysis

The maximum likelihood estimate of the illumination of an image of a natural scene given its mean redness and luminance–redness correlation was determined by means of a linear regression. We adopted as predictors X_1, the mean of the decimal log of r, and X_2, the correlation between log luminance and $\log r$. These predictors could be specified for each of the 12 natural scenes under each of the four illuminants. The optimal weights derived for the prediction of the $\log r$ value of the illuminant ($\hat{Y}$) are embodied in the following linear equation: $\hat{Y} = 1.1305X_1 + 0.0063X_2 + 0.0202$. In deriving the theoretical straight line of Fig. 2b, we assumed that an optimal observer, when confronted with our experimental stimuli, would estimate the redness of the illumination according to this equation in each case and would perceive the resulting estimated illuminant chromaticity as neutral grey, effectively discounting the estimated illuminant in the perception of physically neutral surfaces.

We used the Stockman–MacLeod–Johnson cone sensitivities[30] to calculate all cone excitation values.

Received 27 March; accepted 27 November 2001.

1. Kraft, J. M. & Brainard, D. H. Mechanisms of color constancy under nearly natural viewing. *Proc. Natl Acad. Sci. USA* **96,** 307–312 (1999).
2. Buchsbaum, G. A. Spatial processor model for object colour perception. *J. Franklin Inst.* **310,** 1–26 (1980).
3. Land, E. H. Recent advances in retinex theory. *Vis. Res.* **26,** 7–21 (1986).
4. Gershon, R. & Jepson, A .D. The computation of color constant descriptors in chromatic images. *Color Res. Appl.* **14,** 325–334 (1989).
5. Gilchrist, A. L. & Ramachandran, V. Red rooms in white light appear different from white rooms in red light. *Invest. Ophthalmol. Vis. Sci.* **33,** 756 (1992).
6. Lee, H.-C. Method for computing the scene–illuminant chromaticity from specular highlights. *J. Opt. Soc. Am. A* **3,** 1694–1699 (1986).
7. Tominaga, S. & Wandell, B. A. Standard surface-reflectance model and illuminant estimation. *J. Opt. Soc. Am. A* **6,** 576–584 (1989).
8. D'Zmura, M. & Lennie, P. Mechanisms of color constancy. *J. Opt. Soc. Am. A* **3,** 1662–1672 (1986).
9. Maloney, T. M. & Yang, J. N. in *Colour Perception: From Light to Object* (eds Mausfeld, R. & Heyer, D.) (in the press).
10. Funt, B. V. & Drew, M. S. Color space analysis of mutual illumination. *IEEE Trans. Pattern Anal. Mach. Intell.* **15,** 1319–1326 (1993).
11. Funt, B. V., Drew, M. S. & Ho, J. Color constancy from mutual reflection. *Int. J. Comp. Vis.* **6,** 5–24 (1991).
12. Bloj, M., Kersten, D. & Hurlbert, A. C. Perception of three-dimensional shape influences colour perception through mutual illumination. *Nature* **402,** 877–879 (1999).
13. Bäuml, K.-H. Color appearance: effects of illuminant changes under different surface collections. *J. Opt. Soc. Am. A* **11,** 531–542 (1994).
14. MacLeod, D. I. A., & Golz, J. in *Colour Perception: From Light to Object* (eds Mausfeld, R. & Heyer, D.) (in the press).
15. Mausfeld, R. Color in *Color Vision* (eds Backhaus, W. G. K., Kliegel, R. & Werner, J. S.) 219–250 (De Gruyter, Berlin, 1998).
16. Mausfeld, R. & Andres, J. A reduced variance of receptor codes in chromatic scenes activates a 'discounting the illuminant' mechanism. *Perception* **27** (Suppl.), 42 (1998).
17. Mausfeld, R. & Andres, J. Second order statistics of colour codes modulate transformations that effectuate varying degrees of scene invariance and illumination invariance. *Perception* (in the press).
18. Ruderman, D. L., Cronin, T. W. & Chiao, C. C. Statistics of cone responses to natural images: implications for visual coding. *J. Opt. Soc. Am. A* **15,** 2036–2045 (1998).
19. MacLeod, D. I. A. & Boynton, R. M. Chromaticity diagram showing cone excitation by stimuli of equal luminance. *J. Opt. Soc. Am.* **69,** 1183–1186 (1979).
20. Golz, J. & MacLeod, D. I. A. Influence of scene statistics on color constancy. *Invest. Ophthalmol. Vis. Sci.* **40** (Suppl.), S749 (1999).
21. Eskew, R. T., McLellan, J. S. & Giulianini, F. in *Color Vision: from Genes to Perception* (eds Gegenfurtner, K. R. & Sharpe, L. T.) 345–368 (Cambridge Univ. Press, New York, 1999).
22. Jenness, J. W. & Shevell, S. K. Color appearance with sparse chromatic context. *Vis. Res.* **35,** 797–805 (1995).
23. Brown, R. O. & MacLeod, D. I. A. Color appearance depends on the variance of surround colors. *Curr. Biol.* **7,** 844–849 (1997).
24. Webster, M. A. & Mollon, J. D. Adaptation and the color statistics of natural images. *Vis. Res.* **37,** 3283–3298 (1997).
25. Brainard, D. H. & Freeman, W. T. Bayesian color constancy. *J. Opt. Soc. Am. A,* **14,** 1393–1411 (1997).
26. D'Zmura, M., Iverson, G. & Singer, B. in *Geometric Representations of Perceptual Phenomena* (eds Luce, D., D'Zmura, M., Hoffman, D., Iverson, G. & Romney, A.) 187–202 (Lawrence Erlbaum Associates, Mahwah, 1995).
27. Forsyth, D. A. in *AI and the Eye* (ed. Blake, A. & Troscianko, T.) 201–227 (Wiley, Chichester, 1990).
28. Forsyth, D. A. A novel algorithm for color constancy. *Int. J. Comp. Vis.* **5,** 5–36 (1990).
29. Wyszecki, G., & Stiles, W. S. *Color Science: Concepts and Methods, Quantitative Data and Formulae* 2nd edn 145–146 (Wiley, New York, 1982).
30. Stockman, A., MacLeod, D. I. A. & Johnson, N. E. Spectral sensitivities of the human cones. *J. Opt. Soc. Am. A* **10,** 2491–2521 (1993).

Acknowledgements

We thank D. L. Ruderman, T. W. Cronin and C. C. Chiao for their spectral data of natural scenes. This work was supported by the National Eye Institute. J. Golz was supported by the German–American Fulbright Commission.

Competing interests statement

The authors declare that they have no competing financial interests.

Correspondence and requests for materials should be addressed to J.G. (e-mail: golz@psychologie.uni-kiel.de).

Early consolidation in human primary motor cortex

Wolf Muellbacher*†, Ulf Ziemann*†, Joerg Wissel‡, Nguyet Dang*, Markus Kofler‡, Stefano Facchini*, Babak Boroojerdi*, Werner Poewe‡ & Mark Hallett*

** Human Motor Control Section, Medical Neurology Branch, National Institute of Neurological Disorders and Stroke, National Institutes of Health, Bldg 10, Rm 5N226, 10 Center Drive MSC 1428, Bethesda, Maryland 20892-1428, USA*
‡ Neurological Department, University Hospital of Innsbruck, Anichstrasse 35, A-6020 Innsbruck, Austria

Behavioural studies indicate that a newly acquired motor skill is rapidly consolidated from an initially unstable state to a more stable state[1], whereas neuroimaging studies demonstrate that the brain engages new regions for performance of the task as a result of this consolidation[2]. However, it is not known where a new skill is retained and processed before it is firmly consolidated. Some early aspects of motor skill acquisition involve the primary motor cortex (M1)[3], but the nature of that involvement is unclear. We tested the possibility that the human M1 is essential to early motor consolidation. We monitored changes in elementary motor behaviour while subjects practised fast finger movements that rapidly improved in movement acceleration and muscle force

† Present addresses: Ludwig Boltzmann Institute for Epilepsy and Neuromuscular Disorders, Neurological Hospital of Vienna, Rosenhuegel, Riedelgasse 5, A-1130, Vienna, Austria (W.M.); Clinic of Neurology, JW Goethe University of Frankfurt, Theodor-Stern-Kai 7, D-60590 Frankfurt-am-Main, Germany (U.Z.).